Fabrication and evaluation of PZT/Pt piezoelectric composites and functionally graded actuators

Kenta Takagi[a], Jing-Feng Li[a,b,*], Shohei Yokoyama[a], Ryuzo Watanabe[a]

[a]*Department of Materials Processing, Graduate School of Engineering, Tohoku University, 02, Aoba, Aramaki, Aoba-ku, Sendai, 980-8579, Japan*
[b]*State Key Laboratory of New Ceramics and Fine Processing, Department of Materials Science and Engineering, Tsinghua University, Beijing 100084, PR China*

Abstract

The PZT/Pt composites with various compositions were fabricated by using powder processing, and their mechanical, dielectric, piezoelectric and elastic properties were evaluated with the purpose to develop piezoelectric actuators with functionally graded microstructure (FGM). The piezoelectric and dielectric constants of the PZT/Pt composites decreased monotonously with increasing Pt content, whereas the addition of the Pt particles greatly improved the mechanical properties, particularly the fracture toughness in the composites. Miniature bimorph-type FGM actuators that consist of a composite internal-electrode (70 vol.%PZT/30 vol.%Pt) and three piezoelectric layers (100 vol.%PZT to 80 vol.%PZT/20 vol.%Pt) were fabricated by powder stacking and normal sintering techniques. The electrically-induced deflection characteristics of such an FGM actuator were measured with electric strain gages mounted on the top and bottom surfaces of the actuators, and the measured data were consistent with the analytical results given by the modified classical lamination theory model (CLT).
© 2003 Elsevier Science Ltd. All rights reserved.

Keywords: Actuators; Composites; Functionally graded materials; Piezoelectric properties; PZT

1. Introduction

Piezoelectric actuators and sensors have novel applications for microelectromechanical systems (MEMS)[1,2] and smart material systems,[3] especially in the medical and aerospace industries.[4] A piezoelectric bimorph is a famous type of actuator, in which two piezoelectric ceramic plates are bonded using an organic bonding agent. A positive electric field is applied to one plate while a negative electric field is applied to the other one, so one plate extends while the other one shrinks, resulting in a deflection deformation. Although the piezoelectric bimorph actuators produce large bending displacements, the high stress generated at the interface between two piezoelectric ceramic plates due to a large change of electrically induced strains may cause a premature failure of such a device. The use of bonding agent to form the

bimorph actuators also reduces the reliability of the actuator because it may creep at high temperature or degrade in service.

Functionally graded microstructure (FGM) has been found to relieve high thermal stress at the interface between ceramic and metal plates. Because the introduction of the graded compositions and/or structures leads to the relaxation of stress at the interface, FGM-type actuators are expected to be more reliable than the conventional actuators. Some previous investigations[5,6] have been concentrated on the development of FGM actuators with a graded compositional change from high piezoelectric ceramic to low piezoelectric one, otherwise from low dielectric ceramic to high dielectric one. Analytical studies[7,8] reveal that the graded composition can reduce the stress concentration near the interface. The additional advantage of FGM bimorph actuators is that no bonding agent is needed to bond the piezoelectric ceramic plates, because the piezoelectric layers and the inner electrode can be formed together by sintering process. In FGM piezoelectric ceramic/metal

---

actuators, it is possible to achieve both the gradients of piezoelectric and dielectric constants by using the conductivity of metal phases. In addition, the metal particle dispersions into the piezoelectric matrix can increase the mechanical properties,[9] resulting in improvement in mechanical reliability.

In this study, the lead zirconate titanate (PZT)/Pt system has been selected to develop FGM ceramic/metal bimorph actuator, because PZT is a common type of piezoelectric ceramic and Pt is inert to PZT and oxygen at sintering temperatures. The mechanical, electrical and piezoelectric properties of the PZT/Pt composites were investigated prior to the fabrication of FGM actuators. The PZT/Pt FGM actuators with a symmetrical compositional gradient across the thickness were fabricated, and their electrically induced bending displacement characteristics were evaluated and analyzed by using a modified classical lamination theory.

2. Experimental procedure

The starting materials were commercially available PZT powder (Zr/Ti atomic ratio = 0.516/0.484, average particle size: 0.97 μm, PZT-LQ, Sakai Chemical Industry, Co., Ltd., Japan) as the piezoelectric matrix and platinum powder (average particle size: 3.02 μm, Tanaka Matthey Co., Ltd., Japan) as the metal filler. These powders with a small amount of poly-vinyl-alcohol binder were mixed well using an agate mortar and pestle at compositional ratios of 0–30 vol.% Pt. The mixtures were compacted by die pressing at 100 MPa and cold isostatic pressing (CIP) at 200 MPa. The powder compacts were sintered at 1473 K for 1 h in a covered Al_2O_3 (99.9% purity) crucible containing an excess-PbO atmosphere. Some samples were sintered in a dilatometer to measure the sintering densification behavior.

The sintered microstructure was characterized by scanning electron microscopy (SEM). The fracture strength was measured by a modified small punch (MSP) testing method[10] using a disk specimen of 8 mm in diameter and 0.5 mm thick with one surface being polished to a mirror-like finish. At least five samples were prepared for the fracture strength measurement. The fracture toughness was measured by the indentation micro-fracture (IM) method using a Vickers micro-indenter at a load of 4.9 N. The as-sintered specimens were used for the mechanical tests. To evaluate the piezoelectric and dielectric constants, both surfaces of the specimens were coated with silver pastes and baked at 973 K to form the silver electrodes. The specimens were polarized under an electric field of 1–2 kV/mm in a bath of silicone oil at 393 K. The dielectric and piezo-electric constants and elastic compliances at each composition were measured by using an impedance analyzer (4194A, Hewlett-Packard, US).

The FGM actuator samples consist of seven layers with a center-symmetric composition profile, in which the compositions from the central layer to the surface layer were stepwise changed from 30%Pt to 0%Pt in an interval of 10%Pt. The central 30%Pt layer as an internal electrode was 200 μm thick, and other layers were 300 μm thick. The FGM bimorph actuator was prepared by using a similar process to that for the composites. The mixtures with the corresponding compositions were stacked into a die layer by layer and pressed at 100 MPa. Then the green compacts were CIPed and sintered under the same condition as the composites. The FGM disk-shaped specimens were cut to beams with dimensions of $12 \times 3 \times 2$ mm^3. Then the beam specimens, whose two longitudinal surfaces (12×2 mm^2) were coated with silver paste, were polarized as well as mentioned earlier. Three pieces of conductive wires were attached onto both surfaces and one edge of the internal electrode by using conductive resin. The deflection electrically induced properties of the FGM specimens were evaluated in the voltage range of 100–500 V by using strain gages. The strain gages were mounted along the longitudinal direction on both surfaces. The voltages were supplied to both surfaces by a DC power stabilizer (PMC-500, Kikusui Electronics, Co., Ltd., Japan). The obtained strain values on both surfaces can be converted to the curvature values by using the deflection curve equation as follows:

$$\kappa = \frac{1}{R} = \left(\frac{\varepsilon_1 - \varepsilon_2}{1 + \varepsilon_1}\right) \cdot d_t^{-1} \tag{1}$$

where R and d_t are the radius of curvature and the thickness of actuator. ε_1 and ε_2 are the strain values of the expanding and shrinking sides, whose absolute values should be equal.

3. Results and discussion

3.1. PZT/Pt composites

Sintering densification curves of the pure PZT and its composites containing 15 and 30 vol.%Pt composites are compared in Fig. 1. Both composites begin to shrink at 100° higher temperature than the pure PZT, but the subsequent shrinkage rates were almost the same as the pure PZT. Additionally after being held for 20 min at 1473 K, the shrinkage percentages of all the composites are almost equal to that of the pure PZT. Therefore, the sintering defects such as delamination and warp may not occur in the FGM actuators containing stacked layers of the composites during the sintering process. The relative densities of all the composites sintered at 1473 K for 60 min are above 97.5%, but slightly tend to decrease with increasing Pt content.
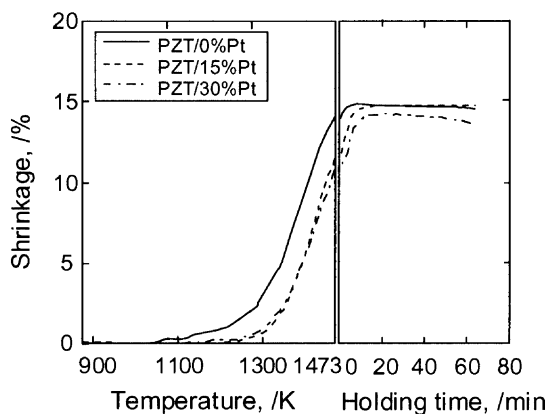
Fig. 1. Sintering shrinkage curves of the monolithic PZT and PZT/Pt composites.

Fig. 2 shows the SEM micrographs of the cross-sections of the PZT/10, 20 and 30 vol.%Pt composites. The gray and white phases in Fig. 2 are the PZT matrices and the Pt particles, respectively. In the 90%PZT/10%Pt composite, Pt particles of hundreds nanometers to several micrometers are uniformly dispersed. As the volume fraction increased, some Pt particles are bonded together to form clusters. At the composition of 30 vol.%Pt, the composite is electrically conductive, indicating that the Pt phase is spatially connected. By X-ray diffraction analysis, it was confirmed that no chemical reaction occurred between the PZT and Pt phases.[11]

The mechanical properties of the composites are strongly dependent on the Pt content, as shown in Fig. 3. The fracture toughness increases as the Pt content increases, because the dispersed ductile Pt particles at crack tips can suppress the crack propagation. Particularly, the irregular Pt clusters effectively resist the crack propagation by crack bridging and deflection mechanisms,[9] thus the fracture toughness improvement is larger in the composite containing more than 20 vol.%Pt addition. On the other hand, the fracture strength increases in the composition range from 0 to 15 vol.%Pt but remains nearly constant when the Pt content exceeds 15 vol.%. This result may be explained by the combination of dispersion-toughening and thermal stress effects. According to Griffith's theory, the increased fracture toughness contributes to an increase in fracture strength, consequently the fracture strength increases with increasing Pt content. However, the thermal residual stress, which is caused by the mismatching of thermal expansion between the PZT matrix and Pt particles, intensified with increasing Pt volume fraction. As a result, the former strengthening effect for the strength is cancelled out by the internal stress, and that is why the strength does not increase furthermore above 15 vol.%Pt.

As shown in Table 1, the piezoelectric and dielectric constants of the composites also greatly depend on the Pt contents. The piezoelectric constants, d_{33} and d_{31}, decrease by the increased addition of Pt particles due to the increased amount of the non-piezoelectric Pt phases. In contrast to this result, the dielectric constant increases with increasing Pt content. An equivalent circuit model composed of R–C parallel elements connected in series can explain such an increase in dielectric constant.[12] It is important for the design of FGM actuators to experimentally measure such compositional dependences of piezoelectric and dielectric constants. The 30
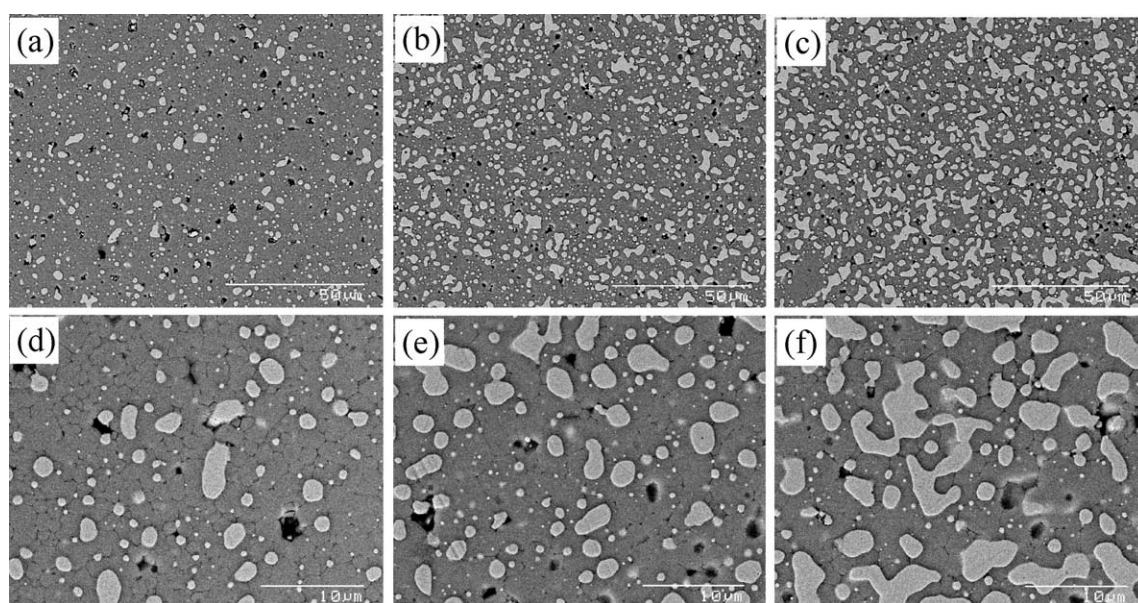

Fig. 2. SEM micrographs showing the dispersion state and connection of Pt particles: (a, d) PZT/10 vol.%Pt composite, (b, e) PZT/20 vol.%Pt and (c, f) PZT/30 vol.%Pt.
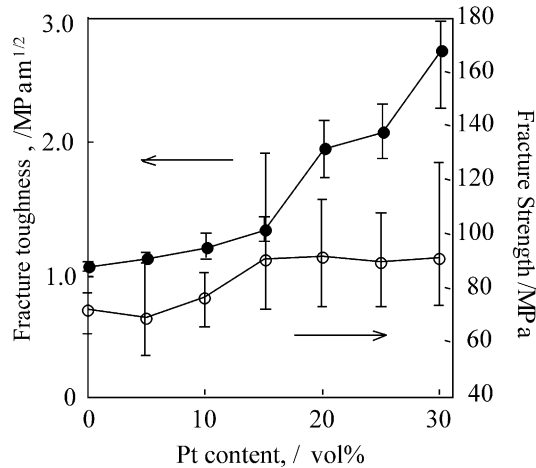
Fig. 3. Enhancement of mechanical properties for PZT ceramic by the Pt particle dispersion: the opened and closed circles show the fracture strength and fracture toughness respectively.
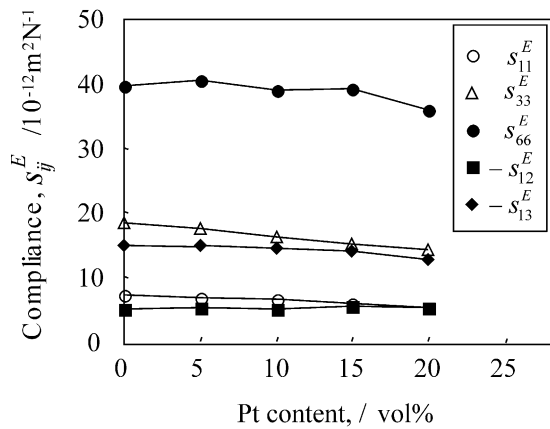
Table 1
Piezoelectric and dielectric constants in the PZT/Pt composites

Pt content (vol.%)	d_{31} $(10^{-10}$ C/m$^2)$	d_{33} $(10^{-10}$ C/m$^2)$	$\varepsilon_{33}/\varepsilon_0$
0	−1.64	3.78	1653
5	−1.51	3.48	1816
10	−1.43	3.25	1959
15	−1.24	2.93	2259
20	−0.98	2.56	2927
30	Conductive	Conductive	Conductive

The PZT/30%Pt composite is not piezoelectric due to the connection of Pt phase

Fig. 4 shows the change in the elastic compliances of the composites as a function of Pt content. The compliances decrease gradually as the Pt content increases, due to the lower elastic constants of Pt. However, the changes are limited, because the elastic constants of PZT and Pt are not so different. As a result, the additions of Pt particle have no significant effects on the elastic constants.

3.2. PZT/Pt FGM actuators

The FGM actuator sample with seven symmetrically laminated layers was prepared based on the above results of the composites. Such a composition combination was selected so that the difference of piezoelectric constants between every adjoining layer can be minimized, in order to avoid a large change of the electrically induced strain. For simplicity, the present sample had a linear composition profile. However, in our previous study[13] it has been realized that the compositional profile can be optimized to obtain the best deflection characteristics and mechanical reliability by numerical design using the property data measured in the present work.

Fig. 5 shows the optical photograph of the FGM actuator specimen. Crack-free and flat FGM samples were prepared with uniform thickness in the length direction. The interfaces between each layer are

Fig. 4. Change of the compliances as a function of Pt content.

vo.l%Pt composite is not piezoelectric or dielectric, but electrically conductive because of percolation of the Pt phase. Therefore, the 30 vol.%Pt composite is expected to act as an internal electrode in the FGM actuators, which are connected well with the neighboring piezoelectric layers without significant thermal stress.
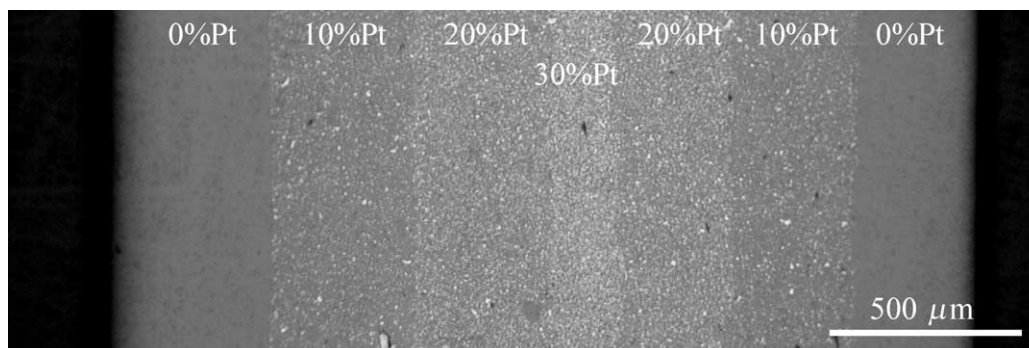

Fig. 5. Optical microscopic photograph of the cross-section of PZT/Pt FGM bimorph actuator. The Pt volume fractions are indicated in the photograph.

smoothly linear and parallel to the surface, and no void was observed at the interfaces. By the image analysis, the thickness of each layer is mostly symmetrical to the middle layer, and the differences of thickness between the actual sample and the designed value are within 50 μm. The microstructure in each layer is the same as the corresponding composite, so the mechanical, electrical and elastic properties of each layer are nearly equivalent to those of the composite.

The electrically induced strains of the FGM actuator were measured, when the voltage of 100–500 V was applied stepwise for 10 s, and the results are given in Fig. 6. The induced strains on both surfaces seem to be proportional to an applied voltage but their polarities are opposite. Thus, a bending mode is generated under an electrical field. The curvatures that are converted by Eq. (1) from the obtained strains values are plotted as a function of the applied voltage in Fig. 7. The curvature values of the FGM and conventional actuators are also compared with the experimental values. The modified classic lamination theory (CLT) given in Appendix A is used here as an analytical model, in which a distribution of the electric field is newly introduced as explained in Appendix B. In this model, the properties of the composites obtained above are used as the properties for each layer. The experimental curvatures are nearly in proportion to the applied voltage. The measured value of curvature at 100 V is 0.0278 m^{-1}, which corresponds to the end-point displacement of 2.0 μm according to the following equation if the beam specimen is assumed as a cantilever.

$$\delta = \frac{1}{2}\kappa l^2 \qquad (2)$$

where δ and l are the displacement and the specimen length, respectively. The experimental results agree with the analytical results when the applied voltage is below
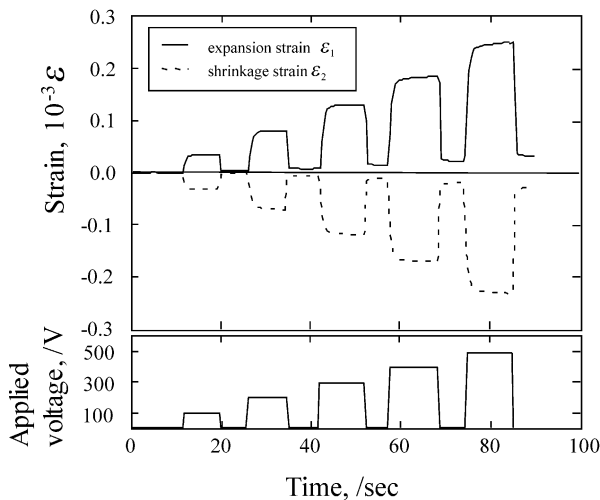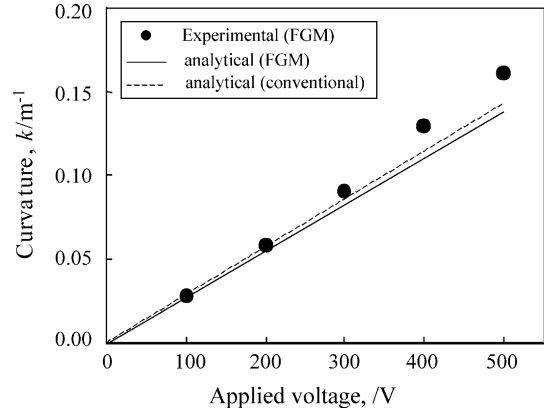

Fig. 7. Relationships between an applied voltage and the curvature in the FGM actuator. The solid and dotted lines show the analytical results of the FGM and conventional bimorph actuators.

300 V, but become increasingly larger than the analytical values when the voltages is above 400 V. This may result from the rotation of some non-180°domains that are induced under a high electric field. In general, the domain switching takes place above electric field of 400–500 V/mm, but it appears that such a critical voltage was lower in the present study. However, when the electric field of 300 V/mm is applied to the whole FGM sample, the electric field applied to the PZT/0%Pt layer will reach 417V/mm, due to the distribution of electric field as described in Appendix B. Furthermore, the curvatures of the FGM bimorph actuator are comparable to the analytical curvatures of a conventional bimorph actuator, which is composed of two PZT layers of 900μm thickness and a PZT/30 vol.%Pt inner electrode layer of 200 μm thickness. Therefore, the introduction of the graded microstructures to a piezoelectric bimorph actuator can not only enhance mechanical reliability but also keep the deflection property at the same level for the conventional bimorph actuators.

4. Conclusion

The properties of the PZT/Pt composites have been investigated with the purpose of developing a PZT/Pt FGM actuator with enhanced mechanical reliability. The addition of the Pt particles into the PZT matrix improves the mechanical properties of the composite. On the other hand, the piezoelectric constants decrease monotonously but the dielectric constant remarkably increases as the Pt content increases. As a result, a bending-type actuator with graded compositions from PZT to PZT/Pt composites can be designed and fabricated by powder processing. FGM actuators obviously generate electrically induced bending displacements, and the values are in agreement with predicted values by the modified lamination theory. The electrically induced

Fig. 6. Electrically induced strains along longitudinal direction on both the faces in the FGM actuator under stepwise applied voltage.

displacement property of the FGM actuator is not inferior to that of the conventional non-FGM actuator.

Appendix A. The modified classic lamination theory

The following model is modified for FGM piezo-electric actuators from the conventional lamination theory by Almajid et al.[7,14] In an infinite piezoelectric plate laminated n layers, the in-plane strain vector at mid-plane, ε^0, and the curvature vector, κ, are expressed as:

$$\begin{bmatrix} \varepsilon^0 \\ \kappa \end{bmatrix} = \begin{bmatrix} A & B \\ B & D \end{bmatrix}^{-1} \begin{bmatrix} N^E \\ M^E \end{bmatrix} \tag{A1}$$

where A, B, D, N^E and M^E are written as:

$$[A, B, D] = \sum_{i=1}^{n} \int_{h_{i-1}}^{h_i} [\overline{Q}]_i (\mathrm{d}z, z\mathrm{d}z, z^2\mathrm{d}z)$$

$$[N, M]^E = \sum_{i=1}^{n} \int_{h_{i-1}}^{h_i} [\overline{e}]_i \{E\}_i (\mathrm{d}z, z\mathrm{d}z) \tag{A2}$$

where h_i is the distance from bottom of the plate to top of the i-th layer. It is noted that $\overline{Q}$ and $\overline{e}$ are the reduced stiffness constant matrix components and reduced piezoelectric constant matrix components, respectively, which are modified from material property matrices due to the assumption of plane stress as given by:

$$\overline{Q}_{ab} = C_{ab} - \frac{C_{a3}}{C_{33}} C_{b3}, \quad \overline{e}_{ab} = \frac{C_{b3}}{C_{33}} e_{33} - e_{ab} \tag{A3}$$

where C_{ab} and e_{ab} are the elastic stiffness and piezoelectric constant, and then the subscripts are given in the well-known Voigt two-index notation. Here the electric field applied to each layer, E, in Eq. (A2) can be worked out by using a multilayer capacitor model.

Appendix B. The distribution of electric field in FGM actuators

It is assumed that the whole body of the laminated plate is a condenser circuit connected in series. The total voltage in the thickness direction, V_t, is given as a sum of voltage of each layer, V_i:

$$V_t = \sum_{i=1}^{n} V_l = Q \sum_{i=1}^{n} \frac{1}{C_i} \tag{A4}$$

where Q is the charge, and C_i is the capacitance of the i-th layer and expressed as:

$$C_i = \frac{\varepsilon_i}{d_i} = \frac{\varepsilon_i}{h_i - h_{i-1}} \tag{A5}$$

where ε_i and d_i are the dielectric constant and thickness of each layer. Substituting Eq. (A5) into Eq. (A4) results in:

$$Q = \frac{V_t}{\sum_{i=1}^{n} \frac{h_i - h_{i-1}}{\varepsilon_i}} \tag{A6}$$

Thus, the electric field in each lamina is obtained by using Eq. (A5) and (A6) as following:

$$E_i = \frac{V_i}{d_i} = \frac{Q}{d_i C_i} = \frac{V_t}{\varepsilon_l \sum_{i=1}^{n} \frac{h_i - h_{i-1}}{\varepsilon_i}} \tag{A7}$$

References

1. Yee, Y., Nam, H.-J., Lee, S.-H., Bu, J. U. and Lee, J.-W., PZT Actuate micromirror for fine-tracking mechanism of high-density optical data storage. *Sensors and Actuators*, 2001, **A89**, 166–173.
2. Wang, S., Li, J.-F., Wakabayashi, K., Esashi, M. and Watanabe, R., Lost silicon mold process for PZT microstructure. *Adv. Mater.*, 1999, **10**, 874–876.
3. Lee, C., Itoh, T. and Suga, T., Self-excited piezoelectric PZT microcantilevers for dynamic SFM with inherent sensing and actuating capabilities. *Sensors and Actuators*, 1999, **A72**, 179–188.
4. Bernhard, A. P. F. and Chopra, I., Trailing edge flap activated by a piezo-induced bending-torsion coupled beam. *J. Am. Helicopter. Soc.*, 1999, **44**, 3–15.
5. Zhu, X. and Meng, Z., Operational principle, fabrication and displacement characteristics of a functionally gradient piezoelectric ceramic actuator. *Sensors and Actuators*, 1995, **A48**, 169–176.
6. Wu, C. C. M., Kahn, M. and Moy, W., Piezoelectric ceramics with functional gradient: a new application in material design. *J. Am. Cream. Soc.*, 1996, **79**, 809–812.
7. Almajid, A., Taya, M. and Hudnut, S., Analysis of out-plane displacement and stress field in a piezoelectric plate with functionally graded microstructure. *Int. J. Solids Struct.*, 2001, **38**, 3377–3391.
8. Kouvatov, A., Steihausen, R., Seifert, W., Hauke, T., Langhammer, H. T., Beige, H. and Abicht, H., Comparison between bimorpic and polymorphic bending devices. *J. Eur. Ceram. Soc.*, 1999, **19**, 1153–1156.
9. Hwang, H. J., Yasuoka, M., Sando, M. and Toriyama, M., Fabrication, sinterability, and mechanical properties of lead zir-

conate titanate/silver compos1ites. *J. Am. Ceram. Soc.*, 1999, **82**, 2417–2422.

10. Li, J.-F., Kawasaki, A. and Watanabe, R., High temperature strength of SiC-AlN solid solutions and composites as evaluation by small punch tests. *J. Jpn. Ins. Met.*, 1992, **56**, 1450–1456.

11. Li, J.-F., Takagi, K., Terakubo, N. and Watanabe, R., Electrical and mechanical properties of piezoelectric ceramic/metal composites in the Pb(Zr,Ti)$_3$/Pt system. *Appl. Phys. Letters*, 2001, **79**, 2441–2443.

12. Phecarroman, C. and Moya, J. S., Experimental evidence of a giant capacitance in insulator-conductor composites at the percolation threshold. *Adv. Mater.*, 2000, **12**, 294–297.

13. Takagi, K., Li, J.-F., Yokoyama, S., Watanabe, R., Almajid, A. and Taya, M., Design and fabrication of functionally graded PZT/Pt piezoelectric bimorph actuator. *Sci. Tec. Adv. Mater.*, 2002, **3**, 217–224.

14. Almajid, A., Taya, M., Takagi, K., Li, J.-F., Watanabe, R., Design and modeling of porous FGM piezoelectric actuators. *Proceeding the 10th US-Japan Seminar on Dielectric and Piezoelectric Ceramics*, Rhode Island, USA, 2001, pp. 309–312.